Extensive Electron-Nuclear Angular Momentum Exchange in Vibrational Autoionization of np and nf Rydberg States of NO

Hongkun Park, David J. Leahy,* and Richard N. Zare
Department of Chemistry, Stanford University, Stanford, California 94305
(Received 13 October 1995)

Vibrational autoionization of individual rotational levels of np ($\nu = 1$) and nf ($\nu = 1$) Rydberg states of nitric oxide (NO) with $11 \leq n \leq 15$ have been studied employing two-color double-resonance excitation via the NO $A\,^2\Sigma^+$ ($\nu_i = 1$) state. The rotational state distributions of the resulting NO^+ $X\,^1\Sigma^+$ ($\nu^+ = 0$) ion have been determined by time-of-flight photoelectron spectroscopy. These measurements show the occurrence of angular momentum exchange between the outgoing electron and the molecular-ion core, a process that has been commonly neglected in theoretical treatments of vibrational autoionization.

PACS numbers: 33.80.Rv, 33.40.+f, 33.80.Eh, 34.80.Kw

Molecular physics often takes for its starting point the separation of nuclear and electronic motion (Born-Oppenheimer approximation) and treats the coupling of these motions by perturbation theory. Vibrational autoionization of a molecule represents a dramatic breakdown of the Born-Oppenheimer approximation in which the vibration of the nuclear framework drives an electron in a Rydberg state above the ionization limit to escape into the continuum [1,2]. As such, vibrational autoionization presents a rare opportunity to study in detail the coupling between the electronic and nuclear motions in a molecule. To date, experimental investigations of this phenomenon have been mostly performed by various spectroscopic techniques, in which positions and widths of Rydberg levels have been measured [3–7]. Multichannel quantum defect theory (MQDT), which is essentially a version of scattering theory, has been shown to be successful in explaining the observed Rydberg-level structures [1,2,8]. Although these experimental and theoretical investigations have yielded valuable insight into the dynamics of vibrational autoionization, a detailed understanding of this process has seldom been accomplished even for a small diatomic molecule owing to the difficulties of probing the final quantum states associated with the ion and the photoelectron.

The NO molecule has served as a benchmark system for the dynamical study of vibrational autoionization of a diatomic molecule, and it has been the subject of numerous experimental and theoretical investigations [9–18]. The level-position analyses of high-lying Rydberg series of NO indicate that the electronic orbital angular momentum quantum numbers l_R of p and f Rydberg electrons are relatively unperturbed [9,10]. The decay dynamics of np and nf Rydberg states are, however, shown to be rather complex because of the interactions between the Rydberg levels and valence electronic states [9,11,12,18], and these NO Rydberg states exhibit competition between vibrational autoionization and predissociation when both channels are open [13,14]. MQDT calculations have been performed to explain various experimental findings [15–18], and they were partially successful in accounting for the observed widths of np Rydberg levels [9,11] and the vibrationally resolved photoelectron angular distributions from vibrational autoionization of nf Rydberg levels [18]. These calculations have explicitly considered the interactions between the Rydberg levels and various valence states but assumed that the orbital angular momentum of the Rydberg electron does not change during the autoionization process [15–18]. As this Letter demonstrates, this last assumption needs revision.

We present rotationally resolved photoelectron spectra from vibrational autoionization of np and nf Rydberg states of NO converging to the NO^+ $X\,^1\Sigma^+$ ($\nu^+ = 1$, N^+) ion. The photoelectron spectra reveal that many rotational levels of NO^+ $X\,^1\Sigma^+$ ($\nu^+ = 0$) are populated after vibrational autoionization of a single rotational level of these Rydberg states. These observations indicate that many different continuum partial waves with electronic orbital angular momentum $\tilde{l}_c$ are produced from the autoionization of nl_R Rydberg states, which sharply contrasts with the behavior of singlet np Rydberg states of H_2 [19], in which the observed rotational state distributions of H_2^+ were consistent with the production of p-partial waves in the ionization continuum. To our knowledge, this study represents the first direct experimental evidence for angular momentum exchange between the Rydberg electron and the molecular-ion core induced by the vibrational quantum change of the core—an effect that has been predicted to occur previously [20,21].

The experimental apparatus has been described in detail elsewhere [22,23]. The essence of our time-of-flight (TOF) photoelectron spectrometer is a magnetically shielded, field-free flight tube. The photoelectrons are produced by intersecting at right angles a molecular beam of NO with two counterpropagating laser beams. The photoelectrons ejected in the direction orthogonal to the plane of the laser beams and the molecular beam are detected using a microchannel plate located 50 cm from the intersection region. The energy resolution of our TOF

spectrometer increases as the energy of the photoelectron decreases; for 200 meV photoelectrons it is approximately 2 meV, which is sufficient to resolve single rotational levels of NO^+ for values of $N^+ \geq 10$.

In the experiment reported here, the *np* ($\nu = 1, N, N_R^+, L$) and *nf* ($\nu = 1, N, N_R^+, L$) Rydberg states of NO converging to the NO^+ $X\,^1\Sigma^+$ ($\nu^+ = 1, N^+ = N_R^+$) ion states are reached by two-color double-resonance excitation via the NO $A\,^2\Sigma^+$ ($\nu_i = 1, J_i = 18.5, N_i = 19$) intermediate level. Both *np* and *nf* Rydberg states of NO ($n > 10$) follow approximately Hund's case (*d*) coupling [5,24,25]. Hence each Rydberg level is designated by angular momentum quantum numbers N, N_R^+, and L: $\vec{N}$ represents the total angular momentum excluding electronic and nuclear spin, $\vec{N}_R^+$ represents the nuclear rotation plus electronic orbital angular momentum for the NO^+ ion core, and L represents the projection of the electronic orbital angular momentum $\vec{l}_R$ on the rotational axis of the core. The distinction between N_R^+ and N^+ should be clearly noted: whereas N_R^+ denotes the rotational angular momentum quantum number of the ion core in the Rydberg states, N^+ denotes the rotational angular momentum quantum number of the bare molecular ion.

Both light beams employed in double-resonance excitation are generated by frequency doubling the outputs of tunable Nd:YAG-pumped dye lasers. The spectral positions of Rydberg levels of NO converging to the NO^+ $X\,^1\Sigma^+$ ($\nu^+ = 1, N^+$) ion were determined by recording the two-color resonance-enhanced multiphoton ionization (REMPI) spectra of NO via the NO $A\,^2\Sigma^+$ ($\nu_i = 1, J_i = 18.5, N_i = 19$) intermediate level in a static gas cell. The first laser was tuned to 213.9 nm to be in resonance with the NO *A-X* (1-0) $R_{21}(17.5)$ line, and the second laser was scanned between the NO^+ $X\,^1\Sigma^+$ ($\nu^+ = 0$) and the NO^+ $X\,^1\Sigma^+$ ($\nu^+ = 1$) ionization thresholds. Over 100 resonance features were observed in the spectrum, each of which could be unambiguously assigned to the *ns*, *np*, and *nf* Rydberg series of NO converging to the NO^+ $X\,^1\Sigma^+$ ($\nu^+ = 1, N^+ = 17{-}21$) ion [26]. A small but typical portion of the spectrum is displayed in Fig. 1 with the assignments for each feature.

Once a resonance feature was assigned, the second laser was tuned to the peak position of a selected Rydberg level, and the photoelectron spectrum was recorded in our photoelectron spectrometer. Typically, the power of the first laser was held below 1 μJ per pulse, whereas that of the second laser was approximately 100 μJ per pulse. The linear polarization vectors of both laser beams were set to be along the flight axis of the photoelectron spectrometer. Under these experimental conditions, the photoionization of NO by the absorption of two successive 213.9 nm photons was minimized, and only photoelectrons that result from the two-color two-photon absorption via the NO $A\,^2\Sigma^+$ ($\nu_i = 1, J_i = 18.5, N_i = 19$) level were observed. These photoelectrons result from the vibrational autoionization of a selected Rydberg level, as evidenced

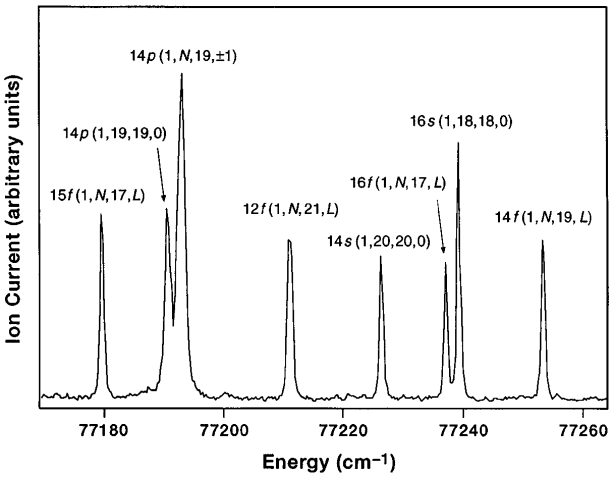

FIG. 1. A typical two-color REMPI spectrum of NO via the NO $A\,^2\Sigma^+$ ($\nu_i = 1, J_i = 18.5, N_i = 19$) level in a static gas cell. The NO pressure in the gas cell is 50 mTorr. Each Rydberg level in the spectrum is denoted by nl_R (ν, N, N_R^+, L). The energy scale is referenced to the $X\,^2\Pi_{1/2}$ ($\nu = 0, J = 1/2$) ground state of NO.

by the observation that no photoelectrons were detected above the noise level when the second laser was tuned off resonance from the position of the Rydberg feature.

Figure 2(a) shows the photoelectron spectrum that results from vibrational autoionization of the $14p$ ($\nu = 1, N = 19, N_R^+ = 19, L = 0$) level, and Fig. 2(b) shows the photoelectron spectrum that results from vibrational autoionization of the $14p$ ($\nu = 1, N, N_R^+ = 19, L = \pm 1$) level. In the latter case, the $14p$ ($\nu = 1, N = 18, N_R^+ = 19, L = -1$) and $14p$ ($\nu = 1, N = 20, N_R^+ = 19, L = 1$) Rydberg levels could not be resolved with the bandwidth of our laser ($\approx$0.5 cm^{-1}) [5,24–26]. Figures 2(c) and 2(d) show the photoelectron spectra obtained from vibrational autoionization of the $14f$ ($\nu = 1, N, N_R^+ = 19, L$) level and the $12f$ ($\nu = 1, N, N_R^+ = 21, L$) level, respectively. Unlike the case in the *np* Rydberg levels, the L substructures of the *nf* Rydberg levels could not be resolved at all as shown in Fig. 1 [5,24–26]. In Figs. 2(a) through 2(d), fully resolved photoelectron peaks that correspond to production of ions in different rotational levels of NO^+ $X\,^1\Sigma^+$ ($\nu^+ = 0$) are clearly discernible. Each photoelectron peak is denoted by the rotational quantum number N^+ of the NO^+ $X\,^1\Sigma^+$ ($\nu^+ = 0$) ion. The value of N^+ associated with each photoelectron peak could be unambiguously assigned in our experiment because the energy calibration of the photoelectron spectrometer was performed by observing photoelectrons from the direct photoionization of the $NO^+ A\,^2\Sigma^+$ ($\nu_i = 1, J_i = 18.5, N_i = 19$) level at an energy above the NO^+ $X\,^1\Sigma^+$ ($\nu^+ = 0$) ionization threshold [23,26].

The photoelectron spectra given in Fig. 2 show that many rotational levels of NO^+ $X\,^1\Sigma^+$ ($\nu^+ = 0$) are populated from vibrational autoionization of *np* ($\nu = 1$) and

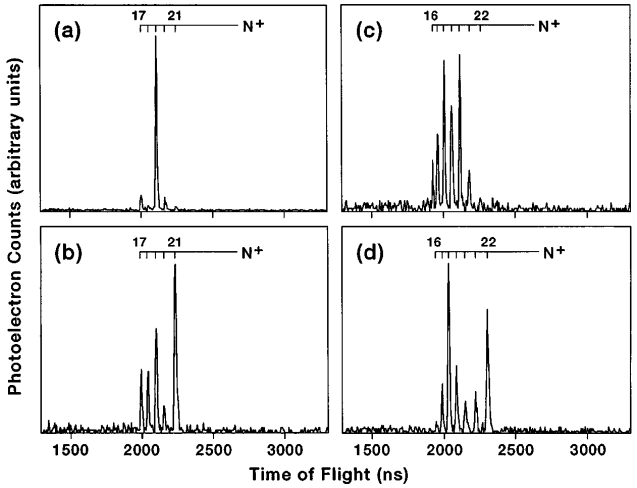

FIG. 2. The time-of-flight photoelectron spectra from vibrational autoionization of (a) the NO $14p$ $(\nu = 1, N = 19, N_R^+ = 19, L = 0)$ level, (b) the NO $14p$ $(\nu = 1, N, N_R^+ = 19, L = \pm 1)$ level, (c) the NO $14f$ $(\nu = 1, N, N_R^+ = 19, L)$ level, and (d) the NO $12f$ $(\nu = 1, N, N_R^+ = 21, L)$ level. In all the spectra N^+ designates the rotational quantum number of NO^+ $X\,^1\Sigma^+$ $(\nu^+ = 0)$ produced by vibrational autoionization of the Rydberg level that has been prepared.

nf $(\nu = 1)$ Rydberg levels with a given rotational quantum number N_R^+. All spectra show several photoelectron peaks with comparable intensities, except for the photoelectron spectrum from vibrational autoionization of the $14p$ $(\nu = 1, N = 19, N_R^+ = 19, L = 0)$ Rydberg level. In addition, inspection of Fig. 2 reveals that the distributions of the ion rotational states produced by autoionization of *np* and *nf* Rydberg levels depend strongly on the quantum numbers L and N_R^+. Especially the rotational state distribution of the NO^+ shown in Fig. 2(d) is remarkably asymmetric around $N^+ = 21$, whereas all the other spectra in Fig. 2 show fairly symmetric intensity patterns around $N^+ = N_R^+ = 19$. A preliminary study shows that this dependence on L and N_R^+ is not restricted to the Rydberg levels investigated here but is a general feature of vibrational autoionization of *nl* Rydberg levels with $11 \leq n \leq 15$ and $l = 0$, 1, and 3 [26].

The observed rotational state distributions of NO^+ provide information on the partial-wave composition of the continuum photoelectrons produced from vibrational autoionization of a given Rydberg level [22,27–30]. The partial-wave composition can be determined from the rotational state distribution of the ion using the photoionization selection rule, $N^+ - N_i + l_c = \text{odd}$, which is applicable to a Σ-Σ photoionization transition [31,32]. The information on the maximum value of l_c can also be inferred from the spectra by using the angular momentum constraint on a Σ-Σ photoionization transition that limits the maximum value of $|N^+ - N_i|$ associated with the l_c-partial wave to be $l_c + 1$ [23]. Note that N_i refers to the rotational quantum number of the intermediate NO A state, which is $N_i = 19$ in our experiment. By applying these considerations to Fig. 2, it can be clearly established that many partial waves with different l_c values are produced by vibrational autoionization of *np* and *nf* Rydberg states converging to the NO^+ $X\,^1\Sigma^+$ $(\nu^+ = 1, N^+)$ ion.

Specifically, the spectrum in Fig. 2(a) shows that mostly p waves are produced by vibrational autoionization of the $14p$ $(\nu = 1, N = 19, N_R^+ = 19, L = 0)$ level, although this figure also shows that a small amount of even partial waves are produced in the ionization continuum. Figure 2(b) indicates that p (and possibly f) waves still dominate the ionization continuum produced by vibrational autoionization of the $14p$ $(\nu = 1, N, N_R^+ = 19, L = \pm 1)$ level. However, the contributions of even partial waves (s and d waves) are more significant in this case compared with vibrational autoionization of the $14p$ $(\nu = 1, N = 19, N_R^+ = 19, L = 0)$ level, as confirmed by the observation of stronger $N^+ = 18$ and $N^+ = 20$ peaks. The photoelectron spectra from vibrational autoionization of *nf* Rydberg states in Figs. 2(c) and 2(d) illustrate, on the other hand, more striking examples of angular momentum exchange between the photoelectron and the ion core induced by the vibration of the molecular core: The intensities of the observed photoelectron peaks indicate that the f waves do not make the largest contribution to the ionization continuum accessed from vibrational autoionization of *nf* Rydberg states. The spectra in Figs. 2(c) and 2(d) are dominated by even N^+ peaks that indicate the dominant production of even (s and d) partial waves in the ionization continuum. The odd (p and f) partial waves nevertheless make significant contributions in the ionization continuum, as signified by the presence of odd N^+ peaks in Figs. 2(c) and 2(d).

As the above discussion illustrates, the photoelectron spectra presented in Fig. 2 provide clear experimental evidence that angular momentum exchange between the photoelectron and the molecular-ion core plays an important role in vibrational autoionization of *np* and *nf* Rydberg states of NO for $11 \leq n \leq 15$. This observation is rather surprising considering that l_R values for both p and f Rydberg electrons are relatively unperturbed [9,10]. In MQDT, the dynamics of vibrational autoionization is governed by the derivatives of the molecule-frame reaction matrix elements, $K_{ll'}(R)$, with respect to R, whereas the level structures of Rydberg states are roughly governed by the vibrationally averaged reaction matrix elements [1,8,33]. Therefore our observation indicates that $dK_{ll'}(R)/dR$ $(l \neq l')$ can be of sizable magnitude even when the vibrationally averaged off-diagonal reaction matrix elements themselves are nearly zero.

As mentioned previously, many experimental investigations have been devoted to the study of vibrational autoionization of NO [9,11–14,18], and several MQDT calculations have been performed to explain these experimental findings [15–18]. The MQDT calculations have shown that both "vibrational" and "electronic"

coupling mechanisms are responsible for the vibrational autoionization of high-lying Rydberg states of NO [15,34]. The vibrational coupling refers to the coupling between the Rydberg states and the nearby ionization continuum caused by the dependence of the electron-ion-core interaction on the internuclear distance R. On the other hand, the electronic coupling refers to the indirect coupling between the Rydberg state and the ionization continuum induced by the strong electronic interactions between the Rydberg and valence states, which is responsible for predissociation of the Rydberg state.

In principle, the angular momentum exchange between the Rydberg electron and the molecular-ion core observed in the present experiment can be explained either by the vibrational coupling mechanism or by the electronic coupling mechanism. In the vibrational coupling mechanism, the angular momentum exchange can be caused by the R dependence of the multipolar interaction between the Rydberg electron and the vibrating-ion core [20,21]. In the electronic coupling mechanism, the partial-wave composition of the continuum electron should depend on the nature of the valence electronic state that is responsible for the indirect coupling. In view of these considerations, the photoelectron spectra given in Fig. 2 indicate that the vibrational autoionization processes of np Rydberg states are mainly governed by the monopolar interaction between the Rydberg electron and the vibrating core, whereas the dipolar interaction makes a significant contribution to vibrational autoionization processes of nf Rydberg states. If both autoionization processes are caused primarily by the electronic coupling mechanism, our experimental observations dictate that distinct electronic states should be responsible for autoionization of np and nf Rydberg states [13–15], because the partial wave compositions produced from the autoionization of np and nf Rydberg states are markedly different. Unfortunately, the rotationally resolved photoelectron spectra presented here are not sufficient to determine alone which of the two mechanisms is primarily responsible for vibrational autoionization processes of the NO np and nf Rydberg states. More work will be necessary to understand these dynamical phenomena, such as the observation of rotationally resolved photoelectron angular distributions and refined MQDT calculations that explicitly consider angular momentum exchange between the outgoing electron and the molecular core [8,33].

We thank J. W. Hepburn for helpful discussions. This work is supported by National Science Foundation under Grant No. NSF PHYS 9320356.

*Present address: Worlds, Inc., 510 Third Street, San Francisco, CA 94107.

[1] C. H. Greene and Ch. Jungen, Adv. At. Mol. Phys. **21**, 51 (1985).
[2] H. Nakamura, Int. Rev. Phys. Chem. **10**, 123 (1991).
[3] G. Herzberg and Ch. Jungen, J. Mol. Spectrosc. **41**, 425 (1972).
[4] Y. Ono *et al.*, J. Chem. Phys. **73**, 4855 (1980).
[5] Y. Anezaki *et al.*, Chem. Phys. **97**, 153 (1985).
[6] M. Schwarz *et al.*, J. Chem. Phys. **89**, 5460 (1988).
[7] C. Bordas *et al.*, Chem. Phys. **129**, 21 (1989).
[8] A. L. Roche and Ch. Jungen, J. Chem. Phys. **98**, 3637 (1993).
[9] E. Miescher, Can. J. Phys. **54**, 2074 (1976).
[10] S. Fredin *et al.*, Mol. Phys. **60**, 825 (1987).
[11] Y. Anezaki *et al.*, Chem. Phys. **89**, 103 (1984).
[12] D. T. Biernacki, S. D. Colson, and E. E. Eyler, J. Chem. Phys. **89**, 2599 (1988).
[13] A. Fujii and N. Morita, Chem. Phys. Lett. **182**, 304 (1991).
[14] A. Fujii and N. Morita, J. Chem. Phys. **97**, 327 (1992).
[15] A. Giusti-Suzor and Ch. Jungen, J. Chem. Phys. **80**, 986 (1984).
[16] M. Raoult, J. Chem. Phys. **87**, 4736 (1987).
[17] K. Nakashima *et al.*, J. Chem. Phys. **91**, 1603 (1989).
[18] J. Guo, A. Mank, and J. W. Hepburn, Phys. Rev. Lett. **74**, 3584 (1995).
[19] S. T. Pratt *et al.*, J. Chem. Phys. **92**, 1831 (1990).
[20] R. S. Berry, J. Chem. Phys. **45**, 1228 (1966).
[21] E. E. Eyler, Phys. Rev. A **34**, 2881 (1986).
[22] S. W. Allendorf *et al.*, J. Chem. Phys. **91**, 2216 (1989).
[23] D. J. Leahy, K. L. Reid, and R. N. Zare, J. Chem. Phys. **95**, 1757 (1991).
[24] J. W. J. Verschuur *et al.*, Chem. Phys. **103**, 359 (1986).
[25] D. T. Biernacki, S. D. Colson, and E. E. Eyler, J. Chem. Phys. **88**, 2099 (1988).
[26] H. Park and R. N. Zare (unpublished).
[27] W. G. Wilson *et al.*, J. Phys. Chem. **88**, 672 (1984).
[28] M.-T. Lee *et al.*, J. Chem. Phys. **96**, 7848 (1992).
[29] D. J. Leahy *et al.*, J. Chem. Phys. **97**, 4948 (1992).
[30] H. Park and R. N. Zare, J. Chem. Phys. (to be published).
[31] S. N. Dixit and V. McKoy, Chem. Phys. Lett. **128**, 49 (1986).
[32] J. Xie and R. N. Zare, J. Chem. Phys. **93**, 3033 (1990).
[33] S. Ross and Ch. Jungen, Phys. Rev. Lett. **59**, 1297 (1987).
[34] A. Giusti-Suzor and H. Lefebvre-Brion, Chem. Phys. Lett. **76**, 132 (1980).